Quantitative Comparison of Cerebral Glucose Metabolic Rates from Two Positron Emission Tomographs

Cheryl L. Grady, Gary Berg, Richard E. Carson, Margaret E. Daube-Witherspoon, Robert P. Friedland, and Stanley I. Rapoport

Laboratory of Neurosciences, National Institute on Aging, NIH; and Department of Nuclear Medicine, Clinical Center, NIH, Bethesda, Maryland

The rapid progress in positron emission tomography technology has created the dilemma of how to compare data from old and new tomographs. We examined cerebral metabolic data from two scanners, with different spatial resolutions and methods of attenuation correction, to see if data from the lower resolution tomograph (ECAT II) could be "corrected" and then compared to data from the higher resolution scanner (Scanditronix PC1024-7B). Nine subjects were scanned on both tomographs after a single injection of [^{18}F]2-fluoro-2-deoxy-D-glucose. Regional and lobar gray matter metabolic rates for glucose were obtained from comparable images from each scanner. Ratios of lobar to global gray matter metabolism also were calculated. Regression coefficients and percent differences were computed to compare ECAT II and PC1024 data. Twenty-four of the 36 regions showed significant regression slopes, and PC1024 measures of glucose utilization ranged from 30% to 120% higher than those from the ECAT II. Lobar differences between the two machines were less variable (50% to 80%), and ratios generally differed by only ±5%. Since there was no simple and consistent relation between regional metabolic rates on the two tomographs, an overall adjustment of regional ECAT values for comparison to PC1024 values would be impossible. A region-by-region adjustment would be necessary. On the other hand, ratios are sufficiently similar that direct comparisons could be made.

J Nucl Med 30:1386–1392, 1989

The technological aspects of positron emission tomography (PET) have evolved rapidly in the last decade, making it likely that an upgrade to a state-of-the-art tomograph will occur during the life of an ongoing research project. If this project is a longitudinal one, the investigators are faced with the problem of how to compare "old" data with "new" data on the same subjects. At the Laboratory of Neuroscience in the National Institute on Aging we have been conducting longitudinal studies of cerebral glucose metabolism in healthy aging and dementia of the Alzheimer type (DAT) since 1981. In 1986 we encountered the situation described above when the NIH PET program replaced the ECAT II tomograph (Ortec, Oak Ridge, TN) (*1*) with a Scanditronix PC1024-7B (Scanditronix, Uppsala, Sweden) (*2*).

Received Nov. 17, 1988; revision accepted Apr. 20, 1989.

For reprints contact: Cheryl L. Grady, PhD, NIA/LNS, Bldg. 10, Room 12S207, 9000 Rockville Pike, Bethesda, MD 20892.

The most obvious difference between the two tomographs is the increased spatial resolution on the PC1024, resulting in increased recovery coefficients, particularly for smaller brain regions, and decreased partial volume effects of cerebrospinal fluid and white matter, as compared with the ECAT II. The PC1024 is a brain scanner with four rings of BGO and GSO crystals (1024 in all), and a transverse field of view that is 26 cm in diameter. The transverse resolution of the PC1024 is 6 mm for straight and cross slices in the center of the field of view. Transverse resolution is degraded by <1 mm at the radial position of the cortex (7 cm). The axial resolution of the PC1024 is 11 and 8 mm for straight and cross slices, respectively, in the center of the field of view, and 11 mm for all slices at the radial position of the cortex. The ECAT II, a whole-body tomograph with a single ring of 66 NaI crystals, has in-plane and axial resolutions of 17 mm in the center of the field of view, which is 50 cm in diameter. In addition to improving resolution, the multi-slice capability of the PC1024

reduces scanning time, thus reducing the influence of k4 on the calculated metabolic rate (*3*), and facilitating the performance of transmission scans for attenuation correction. The PC1024 also has better sensitivity than the ECAT II- 20 and 25k cts/sec/(μCi/cc) for straight and cross slices, respectively, versus 12k cts/sec/(μCi/cc).

All of the above factors will influence the measurements of regional metabolic rates for glucose (rCMRglc) obtained from each machine, making it difficult to predict how metabolic rates obtained from one machine for a particular individual would compare to rates obtained on the same person using the other tomograph. Because of the longitudinal nature of our studies, we thought it important to compare metabolic rates obtained from the two machines on the same individuals to see if a systematic relation could be determined.

There are several ways to compare data from two tomographs. First, in a cross-sectional analysis, one could calculate the global increase in gray matter metabolism obtained with the higher resolution tomograph and adjust the previously obtained regional values upwards. This procedure would be appropriate if there were a linear relation between regional metabolic values from the two tomographs and the variation around the global mean difference was not too great. It also might be possible to track a change in rCMRglc over time in a particular subject. If data from a group of subjects are obtained on both machines, one could calculate the regression of PC1024 values on ECAT values for each region. Using these equations one could predict the value of rCMRglc that would be expected from the new machine given the previously obtained value for an individual not included in the comparison group. If the new obtained value fell outside the confidence limits of prediction, then one could conclude that metabolism had significantly changed. In addition to absolute rCMRglc, normalized values or ratios are routinely used in PET research (e.g., *4,5*). We have shown that some normalized values in individual DAT subjects are stable over time on the ECAT II (*6,7*). It is important to determine if normalized values are similar on the two machines, and whether they are directly comparable, since normalization should remove the effect of any global shift in metabolism.

The present paper presents the results of a series of comparisons that we have made on data obtained from the ECAT II and the Scanditronix PC1024-7B on a sample of subjects, addressing these issues for both absolute rCMRglc and normalized metabolic rates. One approach to this comparison could be to make the data from the two tomographs as similar as possible—(e.g., blurring the PC1024 images to approximate the ECAT II resolution and using only calculated attentuation corrections) to determine the smallest obtainable difference in metabolic values between the two machines. However, we were more interested in this analysis from a practical point of view and thus wanted to compare the data routinely obtained from the new technology to that obtained from the previous methods. Therefore, aside from the change in tomographs, we also instituted transmission scans for attenuation correction and developed new methods of regional analysis (described below) which are included in the present study. An abstract of this work has been published (*8*).

METHODS

Nine subjects participated in the study—seven healthy volunteers (three women and four men, ages 53–90 yr), and two patients (both women, ages 72 and 78 yr) with a diagnosis of probable Alzheimer's disease according to NINCDS-ADRDA criteria (*9*). Subjects were scanned on both tomographs on the same day. Catheters were placed in a radial artery for drawing blood samples and in an antecubital vein for injecting the isotope. Subjects were first placed in the PC1024, with their eyes covered and ears occluded. A line was drawn on the face to define the inferior orbito-meatal (IOM) line, which was used to align the subject in each scanner. Subjects were placed in the PC1024 at 15 mm above the IOM line and a 10-min transmission scan obtained for attenuation correction. Immediately following the transmission scan, a bolus of 5 mCi of fluorine-18-2-fluoro-2-deoxy-D-glucose was injected. Forty-five minutes later one 15-min scan of seven slices was obtained, with at least 2 million counts per slice. The subject then was moved to the ECAT II and the first scan was begun at 15 mm above the IOM line, ~60 min after the isotope injection. Seven slices were obtained on the ECAT II, with the length of each scan adjusted for isotope decay to obtain at least 750,000 counts per slice. The last ECAT scan was completed ~2 hr after the injection.

The seven scans on the ECAT II were obtained at 14 mm steps, thus sampling 101 mm in the axial field of view. The emission data were reconstructed using the medium resolution filter and a calculated attenuation correction was applied to the emission data using an operator-defined ellipse and a coefficient of 0.088 (*4*). The inter-slice distance on the PC1024 is 13.75 mm (center to center), thus including 92.5 mm in the axial field of view, slightly less than that of the ECAT. Emission data from the PC1024 were reconstructed using a 4-mm Bohm filter and were corrected for attenuation using the transmission data. Arterial blood samples were obtained throughout both scans and used for the measurement of blood radioactivity and glucose concentration. Regional cerebral metabolic rates for glucose were calculated using one of two modifications of the operational equation of Sokoloff et al. (*10*)—the Huang equation (*3*) for ECAT II data, or the Brooks equation (*11*) for PC1024 data. These two equations provide essentially the same estimates of rCMRglc (±0.5%, [11]).

ECAT II data were analyzed using the method of Duara et al. (*4*). This method defines brain regions of interest (ROI's) anatomically by comparing the PET images to a standard brain atlas (*12*) and outlining the entire region on the image [see (*13*) for an illustration of these regions]. Mean rCMRglc values (weighted by number of pixels) were calculated for each region over all slices in which it appeared (*4*). PC1024 data

were analyzed using a template composed of 8 mm diameter circles (48 mm^2) spaced evenly throughout the cortical ribbon and centered in subcortical regions. The template for each slice was placed over the matching slice for each subject and adjusted to fit. Regional metabolic rates were obtained by averaging rates in the circular regions that were included in the anatomical location of each ECAT region. For example, in Figure 1 the regions defined as the right superior temporal, caudate and thalamus are outlined on the ECAT image and the five circular regions on the Scanditronix image that were averaged to obtain the right superior temporal value, and the single circles for caudate and thalamus are indicated. Some of the smaller brain regions that are generally seen in only one slice, or regions at the base of the brain, were not available in one or both scans for some individuals due to differences in the relation of the brain to the IOM line among subjects.

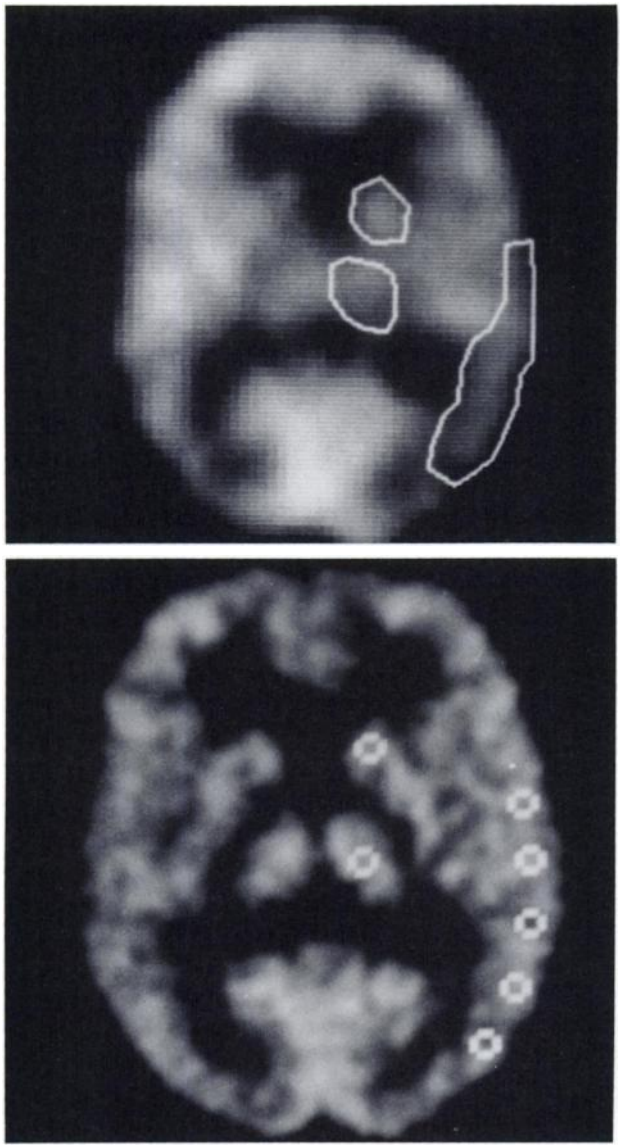

FIGURE 1
Example of ROIs on an ECAT II image (top) and a PC1024 image (bottom). The ROIs used to calculate rCMRglc for the right superior temporal, caudate and thalamus regions are shown on both images.

Thus, for some regions the number of subjects available for statistical comparisons was less than nine (Table 1). All scans were analyzed by the same individual to avoid problems of inter-rater reliability.

Statistical comparisons of rCMRglc from the two tomographs were made in two ways. First, in order to determine the extent of metabolic increase due to increased resolution, percent differences were calculated for the regional values as $[(S-E)/E]\times100$, where S is rCMRglc obtained from the PC1024 and E is rCMRglc obtained from the comparable region on the ECAT II. Regression equations also were calculated for each region, regressing PC1024 rCMRglc on rCMRglc from the ECAT II. Percent differences and regressions also were computed for lobar metabolic rates, which consisted of the mean metabolic rate of all regions in the frontal, parietal, temporal and occipital lobes bilaterally.

For the analysis of normalized metabolic values we used ratios of lobar metabolism to a measure of global metabolism, defined as the mean of all gray matter regions in both hemispheres. We also compared measures of metabolic right/left asymmetry in frontal, parietal and temporal lobes using the formula $(R-L)/[(R+L)/2]$, where R is rCMRglc in a right sided region and L is the value for the homologous region in the left hemisphere. Percent differences were computed on the ratios and absolute values of the asymmetry indices; regression coefficients were calculated on both ratios and asymmetry indices.

RESULTS

The results of the rCMRglc comparisons are shown in Table 1 for both hemispheres. The metabolic rates obtained from the PC1024 were higher than the corresponding values from the ECAT II, ranging from 30% to 122% higher, with a mean elevation of 65 ± 21% (mean ± s.d.) in the right hemisphere and 60 ± 16% in the left. Twenty-four of the 36 pairs of rCMRglc values had regression slopes significantly different from zero. The slopes of the regression equations ranged from −0.1 to 1.9 (mean ± s.d., 1.0 ± 0.3 for the right hemisphere and 1.0 ± 0.4 for the left). There were four regions that failed to show significant regressions in both hemispheres-orbital frontal, primary occipital, and both anterior and posterior medial temporal regions.

Figure 2 shows a plot of PC1024 rCMRglc against ECAT II rCMRglc for the right superior parietal region. The upper and lower 95% confidence limits for prediction also are shown. These data indicate that for a region, such as this one, where the scatter around the regression line is relatively small, one could use the regression equation to predict PC1024 results from ECAT II data for a given subject. For example, if a subject had a metabolic value of 6 mg/100 g/min on the ECAT at time 1, a value of ~8 mg/100 g/min would be expected from the PC1024 at time 2 if no change in metabolism had occurred. However, if a parietal metabolic rate of 5 mg/100 g/min or less were obtained at time 2, metabolism could be said to have declined

TABLE 1
Comparison of Regional Metabolic Results: Absolute Rates, Percent Differences, and Regression Slopes

Region	Right hemisphere				Left hemisphere			
	ECAT II rCMRglc	PC1024 rCMRglc	Δ%	Slope	ECAT II rCMRglc	PC1024 rCMRglc	Δ%	Slope
Prefrontal	5.7 ± 0.9	8.6 ± 1.2	52	1.2 ± 0.2**	5.7 ± 1.0	8.4 ± 1.2	49	1.0 ± 0.3**
Premotor	5.8 ± 0.8	9.1 ± 1.1	57	1.1 ± 0.3**	6.0 ± 1.0	9.2 ± 1.3	53	1.1 ± 0.3**
Orbital frontal*	4.2 ± 0.8	6.9 ± 1.1	75	0.8 ± 0.7	4.4 ± 1.0	7.2 ± 0.8	76	0.5 ± 0.6
Precentral	5.6 ± 1.0	9.3 ± 1.3	67	1.0 ± 0.3†	5.7 ± 1.0	8.9 ± 1.8	56	1.3 ± 0.4†
Postcentral	5.6 ± 0.9	8.6 ± 1.3	56	1.1 ± 0.3†	5.7 ± 1.0	8.1 ± 1.2	44	0.9 ± 0.3†
Superior parietal	5.5 ± 1.1	8.2 ± 1.6	50	1.1 ± 0.4†	5.4 ± 1.1	7.9 ± 1.4	47	1.1 ± 0.3†
Inferior parietal	5.4 ± 0.6	8.4 ± 1.2	57	1.2 ± 0.5	5.4 ± 0.8	8.3 ± 1.2	55	1.1 ± 0.4†
Occipital association	5.1 ± 0.8	8.4 ± 1.0	66	0.8 ± 0.4	5.0 ± 0.7	8.6 ± 0.9	73	0.8 ± 0.3†
Primary occipital	5.8 ± 0.9	9.3 ± 1.3	62	0.7 ± 0.5	5.8 ± 0.7	9.3 ± 1.2	62	0.6 ± 0.6
Superior temporal	5.1 ± 0.7	8.5 ± 0.9	70	1.0 ± 0.4†	5.4 ± 0.8	8.4 ± 1.1	57	1.1 ± 0.3**
Middle temporal*	3.8 ± 0.5	7.8 ± 0.8	110	1.5 ± 0.7	4.3 ± 0.7	7.6 ± 1.0	85	1.9 ± 0.5**
Inferior temporal†	3.2 ± 0.6	6.6 ± 0.6	122	0.7 ± 0.2	3.6 ± 0.5	6.2 ± 0.9	97	1.6 ± 0.1**
Anterior medial temporal‡	3.8 ± 0.5	5.5 ± 0.7	44	0.5 ± 0.8	4.0 ± 0.6	5.9 ± 0.6	47	−0.1 ± 0.8
Posterior medial temporal§	4.6 ± 0.5	7.0 ± 0.9	55	0.5 ± 0.7	4.8 ± 0.6	6.9 ± 0.7	48	0.3 ± 0.4
Caudate nucleus	6.3 ± 1.2	10.1 ± 1.5	63	1.1 ± 0.2**	6.4 ± 1.5	10.4 ± 1.8	65	1.1 ± 0.2**
Thalamus	5.8 ± 1.0	9.7 ± 1.8	69	1.3 ± 0.4†	5.9 ± 1.1	9.6 ± 1.8	65	1.2 ± 0.4†
Lenticular nucleus	6.4 ± 1.4	10.2 ± 1.4	63	0.8 ± 0.2**	6.5 ± 1.5	10.6 ± 1.8	64	1.0 ± 0.2**
Insula	6.1 ± 0.7	8.3 ± 0.9	36	0.9 ± 0.3†	6.4 ± 1.0	8.3 ± 1.0	30	0.8 ± 0.2†

Metabolic rates are mean ± s.d. (mg/100g/min); slopes are slope ± s.e.
Δ% = [(PC1024-ECAT II)/ECAT II] × 100; * N = 8; † N = 4; ‡ N = 6; § N = 7.
† $p < 0.05$; ** $p < 0.01$.

significantly, since a value this low falls below the lower 95% confidence limit for prediction for this region.

The lobar results are shown in Table 2. PC1024 metabolic rates ranged from 50% to 80% higher than the ECAT II data (mean ± s.d., 63 ± 13% for the right hemisphere and 59 ± 8% for the left), a range which was half that seen in the regional comparison. All but one region (right lateral temporal) showed a significant regression. The slopes also showed a smaller range as compared to the slopes of regional values, varying from 0.8 to 1.2 (mean ± s.d., 1.0 ± 0.2 for the right hemisphere and 1.1 ± 0.1 for the left), and showed consistently small standard errors.

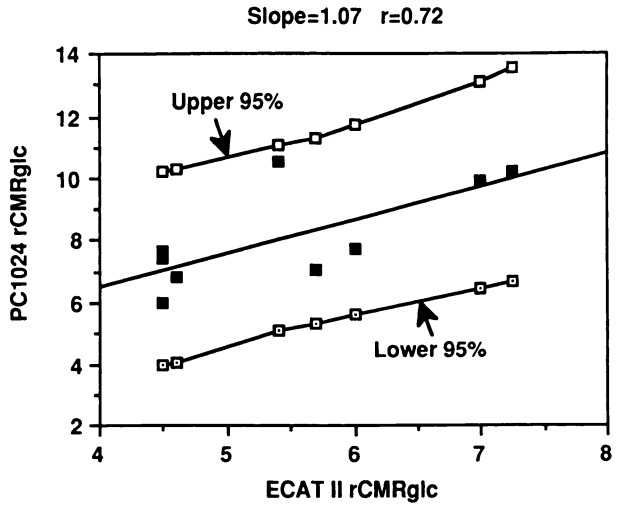

FIGURE 2
PC1024 rCMRglc plotted against ECAT rCMRglc for the right superior parietal region. The best-fit regression line and the upper and lower 95% confidence limits for prediction are shown.

The differences between the two sets of ratios (Table 2) ranged from −5% to 5% for frontal, parietal and occipital regions, a much smaller difference than was found for absolute rCMRglc. The percent difference from the temporal ratios was somewhat larger, particularly the right temporal/global ratio (16%). Two ratios had statistically significant regressions (Table 2). The left temporal/global ratio is shown in Figure 3 along with the left frontal/global ratio for comparison. Percent differences between the asymmetry indices (Table 2) were quite large because these measures generally have very small values (close to zero) and a very small change can result in a large percent difference. The parietal asymmetry index (Fig. 4) was the only asymmetry index to show a significant relation between the two tomographs.

DISCUSSION

We found rCMRglc to be higher overall in data from the high resolution Scanditronix PC1024, as compared with the lower resolution ECAT II. The percent increase in rCMRglc was greatest in those regions with the lowest values from the ECAT II, which probably were the ones most affected by both partial volume artifact and inadequate attenuation correction, and thus underesti-

TABLE 2
Comparison of Lobar Metabolic Rates, Ratios, and Asymmetry Indices

Region	Right hemisphere				Left hemisphere			
	ECAT II	PC1024	Δ%	Slope	ECAT II	PC1024	Δ%	Slope
A. Lobar rCMRglc								
Frontal	5.4 ± 0.8	8.8 ± 1.1	63	1.2 ± 0.2‡	5.6 ± 1.0	8.8 ± 1.2	59	1.0 ± 0.3‡
Parietal	5.4 ± 0.8	8.1 ± 1.2	51	1.1 ± 0.4*	5.4 ± 0.9	8.0 ± 1.3	48	1.2 ± 0.3‡
Occipital	5.5 ± 0.7	8.6 ± 1.0	58	1.0 ± 0.4*	5.4 ± 0.6	8.7 ± 0.9	63	1.2 ± 0.2‡
Lateral Temporal	4.4 ± 0.6	7.9 ± 0.8	81	0.8 ± 0.4	4.7 ± 0.7	7.8 ± 1.0	67	1.1 ± 0.4*
B. Ratios to mean gray rCMRglc								
Frontal	0.99 ± 0.02	1.03 ± 0.04	5	1.1 ± 0.7	1.01 ± 0.05	1.02 ± 0.05	2	0.2 ± 0.4
Parietal	0.99 ± 0.05	0.96 ± 0.10	−3	1.3 ± 0.5*	0.99 ± 0.04	0.93 ± 0.05	−5	0.7 ± 0.4
Occipital	1.00 ± 0.07	1.01 ± 0.08	1	0.6 ± 0.4	0.98 ± 0.05	1.03 ± 0.05	5	0.4 ± 0.3
Lateral Temporal	0.80 ± 0.03	0.93 ± 0.05	16	0.0 ± 0.7	0.85 ± 0.05	0.91 ± 0.09	7	1.2 ± 0.5*
C. Right/left asymmetry indices								
Frontal	0.00 ± 0.01	0.01 ± 0.06	657	2.7 ± 1.6				
Parietal	0.00 ± 0.01	0.02 ± 0.10	518	6.0 ± 1.5‡				
Temporal	−0.01 ± 0.02	0.02 ± 0.10	392	3.0 ± 1.5				

Metabolic indices are mean ± s.d.; Slopes are slope ± s.e.; N = 9 in all comparisons.
Δ% = [(PC1024-ECAT II)/ECAT II] × 100.
* $p < 0.05$; ‡ $p < 0.01$.

mated the most. If rCMRglc from the higher resolution machine is assumed to be closer to the true metabolic rate, then the absence of a significant relation between the two tomographs for medial temporal, primary occipital, and orbital frontal regions is an indication of how poorly these areas are imaged with low resolution tomographs. The use of two different ROI methods would have the effect of increasing the difference between the two tomographs, since outlining a region (as was done on the ECAT II data) would include radioactivity from surrounding tissue and increase the partial volume artifact, whereas sampling a small region of gray matter (as was done on the PC1024 data) would reduce such artifact. This effect of ROI methodologies might affect small or thin regions more than large regions, since, in large regions most of the radioactivity would be recovered by both tomographs (*14,15*) and the estimate of rCMRglc more similar regardless of the method of ROI analysis. Although some of the variability in percent difference between the two tomographs may be the result of the ROI analyses, examination of Table 1 does not reveal any clear relation between region size and percent difference.

These results show clearly that for regional rCMRglc values, the considerable variability in percent difference (30% coefficient of variation) precludes the application of a single "correction factor" that can be applied to all ECAT II values to bring them into the range of values from the PC1024. Each regional value would need to be adjusted individually. Although some regions do not show a significant relation between scanners, this would not necessarily mean that adjustment is impossible. For example, even with a slope near zero one could accurately calculate the PC1024 value from the ECAT value (or vice versa) using the regression equation as long as the standard errors of the parameter estimates were not large. However, the regions with nonsignificant slopes also tended to have larger standard errors, increasing the uncertainty in using these estimates.

There was, therefore, no simple interaction between the complex structure of the brain and the differences in performance characteristics of the two tomographs. Using larger regions, such as lobes, resulted in less variability in all comparison measures. The lobar rates could be adjusted using a global measure of percent difference or a global regression equation, although there would be some underestimation in temporal regions.

Another use of these data is in the determination of significant changes in metabolism obtained at follow-up using the regression equation for each region or lobe. This would be feasible for many regions, particularly those that are known to be affected in DAT, such as the parietal, premotor and superior temporal areas (*16–19*). These regions show significant regressions between tomographs and reasonably small standard errors of the slopes in both hemispheres, so that the confidence limits of prediction could be used to test for significant changes in longitudinal data.

In addition to the issue of longitudinal comparisons within a laboratory, the data presented here also illustrate the difficulty in directly comparing metabolic rates

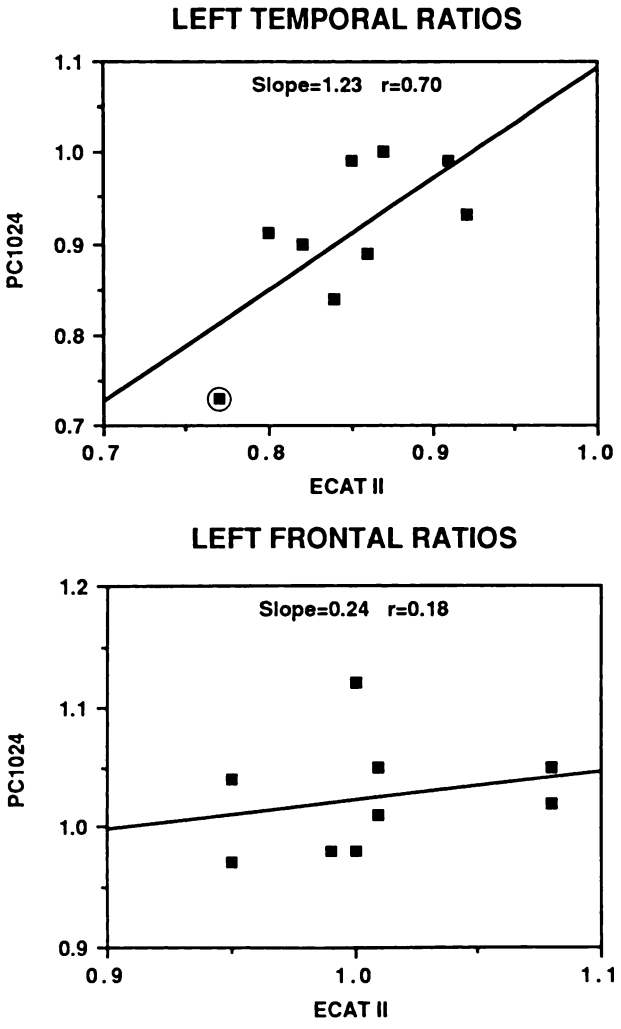

FIGURE 3
Ratios of lobar rCMRglc to mean gray rCMRglc for two regions in the left hemisphere are shown, with PC1024 values on the ordinate and ECAT values on the abscissa. The circled data point in the graph of left temporal ratios represents data from one of the DAT patients (see text).

obtained from different laboratories, in which the scanning procedures, as well as the tomograph used, are often different. Metabolic rates for gray matter in healthy subjects reported in the literature range from 5 mg/100 g/min (*4*) to over 7 mg/100 g/min (*20, 21*), and the values reported here of 5.5 (ECAT II) and 8.5 mg/100 g/min (PC1024) represent a still greater range. If a difference of 3 mg/100 g/min can be obtained on the same subjects with the same injection using different tomographs, then apparent differences in metabolic rates reported by different groups should be interpreted with caution.

Ratios of regional to global CMRglc are sufficiently similar between tomographs (generally within ± 5%) that these measurements could be compared directly, although again there would be somewhat more error in comparing the temporal regions. The temporal ratios are generally higher on the PC1024, due to the increased asymmetry indices is found consistently.

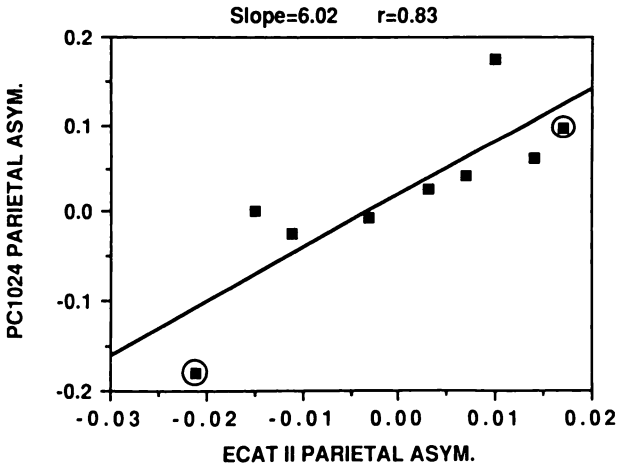

FIGURE 4
The parietal asymmetry index plotted for PC1024 (ordinate) and ECAT (abscissa). Positive values of the index indicate disproportionate left hemisphere hypometabolism and negative values indicate disproportionate right hemisphere hypometabolism. The data points from the two DAT patients are circled.

accuracy of measurement discussed above. However, as can be seen in Figure 3 for the left frontal lobe, in other regions of the brain the range of ratio values is almost identical for the two sets of data. The absence of a significant slope between the ratio values from the two tomographs probably is due to the restricted range of data, as most values cluster around 1.0. One DAT patient fell outside the cluster in the left temporal and right parietal data, accounting for the significant regressions in these ratios.

The asymmetry indices also have a restricted range of values, as most of the indices on both tomographs cluster around zero. This accounts for the lack of relation of these indices except for the parietal index (Fig. 4), where the variability was sufficient to result in a significant slope. The two DAT patients (indicated in the figure) fall at or near the extreme ends of the distribution, as one would expect, given previous findings of greater metabolic asymmetry in this population compared to healthy aged individuals (*5,16,18,22,23*). This suggests that the earlier findings of increased asymmetry in DAT will be replicated with higher resolution tomographs. From Fig. 4 and Table 2 it appears that even the healthy subjects show a somewhat greater range of asymmetry values on the PC1024 than on the ECAT II. Whereas this may be due to less blurring of the PC1024 images, absolute asymmetry values of 0.20 to 0.30 have been reported in DAT patients (*24*). The study of larger groups of patients and controls on the PC1024 will indicate whether an increased range of

ACKNOWLEDGMENTS

The authors thank the following individuals for their assistance in conducting this study: Michael Green, Paul Bald-

win, Gerard Jacobs, Stacey Stein, Brian Petrie, Robert Weltman, and Sven Holte.

REFERENCES

1. Williams CW, Crabtree MCC, Burgiss SG. Design and performance characteristics of a positron emission axial tomograph-ECAT II. *IEEE Trans Nucl Sci* 1979; NS-26:619–627.
2. Daube-Witherspoon ME, Green MV, Holte S. Performance of Scanditronix PC1024-7B PET scanner [Abstract]. *J Nucl Med* 1987: 28:607–608.
3. Huang SC, Phelps ME, Hoffman, EJ, Sideris K, Selin CJ, Kuhl DE. Non-invasive determination of local cerebral metabolic rate of glucose in man. *Am J Physiol* 1980; 238:E69–E82.
4. Duara R, Grady CL, Haxby JV, et al. Human brain glucose utilization and cognitive function in relation to age. *Ann Neurol* 1984; 16:702–713.
5. Haxby JV, Grady CL, Duara R, Schlageter NL, Berg G, Rapoport SI. Neocortical metabolic abnormalities precede nonmemory cognitive defects in early Alzheimer's-type dementia. *Arch Neurol* 1986; 43:882–885.
6. Grady CL, Haxby JV, Schlageter NL, Berg GW, Rapoport SI. Stability of metabolic and neuropsychological asymmetries in dementia of the Alzheimer type. *Neurology* 1986; 36:1390–1392.
7. Grady CL. Longitudinal changes in brain metabolism. pp. 302–304. In: Friedland RP, moderator. Alzheimer disease: clinical and biological heterogeneity. *Ann Int Med* 1988; 109:298–311.
8. Grady CL, Berg G, Carson RE, Daube-Witherspoon ME, Friedland RP, Rapoport SI. Quantitative comparison of glucose metabolic rate from two positron emission tomographs [Abstract]. *J Nucl Med* 1988; 29:867.
9. McKhann G, Drachman D, Folstein M, Katzman R, Price D, Stadlan EM. Clinical diagnosis of Alzheimer's disease: report of the NINCDS-ADRDA work group under the auspices of Department of Health and Human Services task force on Alzheimer's disease. *Neurology* 1984; 34:939–944.
10. Sokoloff L, Reivich M, Kennedy C, et al. The [14C]-deoxyglucose method for the measurement of local cerebral glucose utilization: theory, procedure and normal values in the conscious and anesthetized albino rat. *J Neurochem* 1977; 28:897–916.
11. Brooks RA. Alternative formula for glucose utilization using labeled deoxyglucose. *J Nucl Med* 1982; 23:538–539.
12. Eycleshymer AC, Shoemaker DM. A Cross-section anatomy. New York: Appleton and Co.: 1911.
13. Rumsey J, Duara R, Grady CL, et al. Brain metabolism in autism: resting cerebral glucose utilization rates as measured with positron emission tomography (PET). *Arch Gen Psychiat* 1985; 42:448–455.
14. Hoffman EJ, Huang S-C, Phelps ME. Quantitation in positron emission computed tomography: 1. Effect of object size. *J Comp Assist Tomogr* 1979; 3:299–308.
15. Mazziotta JC, Phelps ME, Plummer D, et al. Quantitation in positron emission computed tomography: 5. Physical-anatomical effects. *J Comp Assist Tomogr* 1981; 5:734–743.
16. Duara R, Grady CL, Haxby JV, et al. Positron emission tomography in Alzheimer's disease. *Neurology* 1986; 36:879–887.
17. Haxby JV, Grady CL, Koss E, et al. Heterogeneous anterior-posterior metabolic patterns in Alzheimer's type dementia. *Neurology* 1988; 38:1853–1863.
18. Friedland RP, Budinger TF, Koss E, Ober BA. Alzheimer's disease: anterior-posterior and lateral hemispheric alterations in cortical glucose utilization. *Neurosci Lett* 1985; 53:235–240.
19. Foster NL, Chase TN, Mansi L, et al. Cortical abnormalities in Alzheimer's disease. *Ann Neurol* 1984; 16:649–654.
20. Brooks RA, Hatazawa J, Di Chiro G, et al. Human cerebral glucose metabolism determined by positron emission tomography: a revisit. *J Cereb Blood Flow Metab* 1987; 7:427–432.
21. Jagust W, Friedland RP, Budinger TF. Positron emission tomography with [^{18}F]fluorodeoxyglucose differentiates normal pressure hydrocephalus from Alzheimer-type dementia. *J Neurol Neurosurg Psychiatr* 1985; 48:1091–1096.
22. Foster NL, Chase TN, Fedio P, et al. Alzheimer's disease: focal cortical changes shown by positron emission tomography. *Neurology* 1983; 33:961–965.
23. Haxby JV, Duara R, Grady CL, et al. Relations between neuropsychological and cerebral metabolic asymmetries in early Alzheimer's disease. *J Cereb Blood Flow Metab* 1985; 5:193–200.
24. Grady CL, Haxby JV, Horwitz B, et al. Longitudinal study of the early neuropsychological and cerebral metabolic changes in dementia of the Alzheimer type. *J Clin Exp Neuropsychol* 1988; 10:576–596.